

Interface structure and misfit dislocations in thin Cu films on Ru(0001)

G. O. Pötschke and R. J. Behm

*Institute für Kristallographie und Mineralogie, Universität München, Theresienstrasse 41,
W-8000 München 2, Federal Republic of Germany*

(Received 4 February 1991)

We show, from scanning tunneling microscopy measurements, that the strain at the interface between Cu films and a Ru(0001) substrate is reduced by a structural transformation from a more tightly bound, strained pseudomorphic first Cu layer to a unidirectionally contracted second Cu layer with periodic partial misfit dislocations. These results for a two-dimensional structure confirm the mechanism of stress accommodation in strained layers predicted in the one-dimensional dislocation model of Frank and van der Merwe.

The structure of ultrathin metal films epitaxially grown on metallic substrates represents a delicate balance between the lattice geometry imposed by the substrate and the (bulk) geometry of the respective film material. The mismatch between these two lattices leads to strain in the first layers of the film, until the film lattice has adopted its bulk geometry. Following earlier (one-dimensional) model calculations the lattice strain is reduced and is finally removed by sequences of dislocations in the film layers.¹ The existence of these dislocations was first verified by electron microscopy,² but it had not been possible to unravel the exact (two-dimensional) nature of the structural transition between the respective lattices. In this Rapid Communication we report results of a scanning tunneling microscopy (STM) study on the structure and growth of Cu films on a Ru(001) substrate, which give direct access to the periodic and defect structure of the first Cu layers and thus to the nature of structural transition in the interface region.

Previous investigations of this system using integrating techniques resulted in partly differing findings. Christmann, Ertl, and Shimizu³ reported a disordered Cu adlayer in the submonolayer regime and a Cu(111)-like structure for three-dimensional agglomerates at higher coverages, while later studies by Houston *et al.*⁴ and Park, Bauer, and Poppa⁵ agreed on the formation of two-dimensional, pseudomorphic islands in the first layer and an epitaxial Cu(111) structure for the second layer. The latter authors also found a slight rotation of 1.8° of the hexagonal lattice of the second layer with respect to that of the substrate.⁵

The STM measurements were performed in an ultrahigh-vacuum STM with *in situ* facilities for ion sputtering, Auger-electron spectroscopy (AES), low-energy electron diffraction (LEED), and thermal desorption spectroscopy (TDS). Nominal Cu coverages were determined by AES and TDS. STM images are shown in a top-view representation, with darker shades corresponding to lower levels. Details of the experimental setup conditions are described elsewhere.⁶

The clean and well-annealed Ru(0001) surface forms extremely large, atomically flat terraces, which often extend over more than 1000 Å in width and are separated by monoatomic, linear steps with very low kink densities.

Upon deposition at room temperature, Cu adatoms condense into islands of one-layer thickness (ca. 2.1 Å in height) even at the lowest coverages. The islands are often attached to steps on the Ru substrate (2.14 Å in height). By STM we found no measurable corrugation on these islands, independent of coverage. The onset of second-layer nucleation, on top of the first-layer areas, depends sensitively on the deposition or annealing temperature, as reported in Ref. 6.

The structure and topography of a Cu film of nominally 1.3 monolayers, deposited at 300 K and subsequently annealed to 520 K, are illustrated in the STM image in Fig. 1(a). (No indications of interdiffusion were found in the entire temperature range up to desorption.³⁻⁵) The imaged surface area contains three different terrace levels, distinguished by their different grey shades in the image. The uppermost level (light grey) consists of two separate

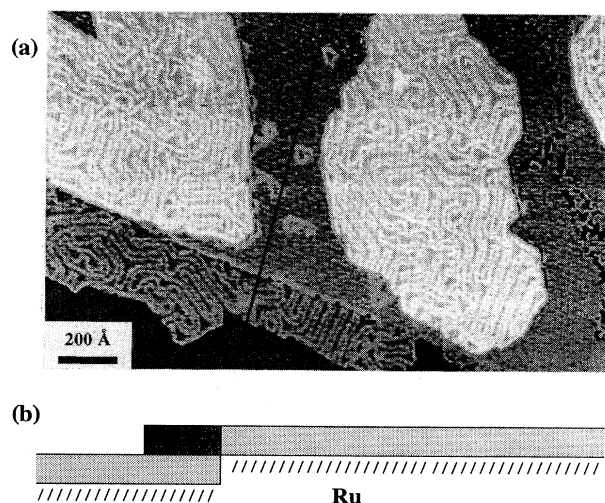


FIG. 1. (a) STM topograph of a Cu-covered Ru(0001) surface ($\Theta_{\text{Cu}}=1.3$, $T_{\text{ann}}=520$ K, 1950×1350 Å²) exhibiting three terrace levels (colored light, medium, and dark). A characteristic corrugation on part of the surface and structural defects are resolved. (b) Film/substrate morphology along the line indicated in (a) (Ru substrate: *//////*; 1st Cu layer: *———*; 2nd Cu layer: *■■■*).

islands of about 500–1000 Å in diameter plus a small part of a third island at the upper-right corner of the image. In contrast to the first-layer Cu islands described previously, these islands exhibit a characteristic corrugation which is dominated by slightly elevated, parallel lines. The lines are frequently found in a pairwise arrangement. Three preferred directions approximately 120° apart can be identified. Further details of this structure are discussed after presentation of Fig. 3.

The middle-terrace level (medium grey) includes two different phases. The larger fraction exhibits no corrugation, comparable to the structure in the first Cu-layer islands, while a smaller area in the foreground shows a corrugation pattern similar to that of the islands in the uppermost level of this image (light grey). (The apparent two-dimensional corrugation in the “noncorrugated” area is an experimental artifact resulting from instabilities in the measurement.) Two different types of structural defects are observed in this area. A number of deep holes (ca. 1–2-Å depth), connected in an extended “chain,” is resolved at the right-hand side of the image. Additional small defect structures of 100–150 Å in diameter exist in the region between the two islands. Finally, the structure of the lowest-terrace level (dark grey, foreground) is identical to that of the uncorrugated phase on the middle-terrace level.

Based on the nominal coverage, the uncorrugated and the corrugated surfaces are associated with a monolayer and a bilayer Cu film, respectively. This assignment was confirmed by STM measurements using an oxygen labeling technique, which allowed an unambiguous distinction between the Ru(0001) substrate and a pseudomorphic Cu adlayer. Following oxygen exposure we could resolve the characteristic corrugation of the $p(2 \times 2)O$ structure on bare Ru(0001) areas, while there is negligible adsorption on the Cu-covered areas. Hence the entire area of this image is covered by at least one Cu layer. The islands in the uppermost level represent second-layer Cu islands on a closed Cu monolayer. The existence of two different structures in the middle-terrace level is caused by an underlying step in the Ru substrate, as shown in the schematic cut in Fig. 1(b). At the phase boundary a (noncorrugated) first Cu layer on the upper terrace of the Ru substrate meets a (corrugated) second Cu layer on the lower terrace of the substrate. The phase boundary proceeds almost linearly over more than 1000 Å, very much like steps on clean Ru surfaces and in agreement with the above assignment. The island perimeters, in contrast, are more irregular.

The absence of any additional corrugation in STM images of the first Cu layer agrees well with the pseudomorphic (1×1) structure derived from LEED observations.^{4,5} The deep holes in the middle level are associated with missing atoms in the first Cu layer. They presumably mark the boundary between two former first-layer islands, which have not completely coalesced. Following room-temperature deposition, such holes were observed up to nominal coverages of 3 ML. They are remarkably stable and were seen even after annealing to 1000 K.

The other structural defects in the first layer exhibit a characteristic triangular shape, which is resolved in more

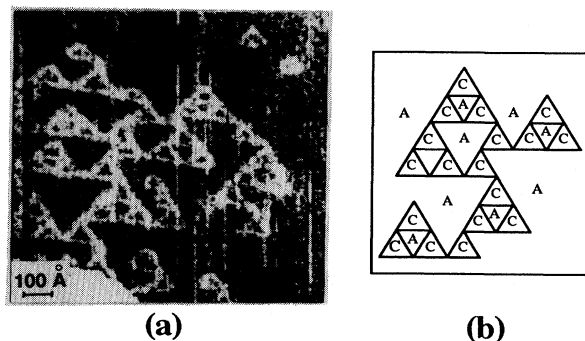


FIG. 2. Defect structure in the first Cu layer on Ru(0001) ($\Theta_{Cu} = 1.3$ ML, $T_{ann} = 520$ K). (a) STM topograph (ca. 1100×1100 Å²) resolving a characteristic network of prominent triangles; (b) schematic model indicating the stacking type of Cu atoms in the triangles; A: hcp stacking; C: fcc stacking.

detail in the STM image in Fig. 2. These triangles are formed by slightly elevated lines, ca. 15–20 Å wide and 0.2–0.5 Å high, which very much resemble the lines in the second Cu layer described above. Their sides coincide with the close-packed [100] directions of the substrate, normal to the direction of the line pairs in the second Cu layer. The orientation of the triangles is constant within the terraces, but changes by 180° between subsequent Ru terraces. The average edge length of these triangular structures is 50–100 Å, and was never observed to exceed 150 Å. Instead, they cluster to form networks which again exhibit a triangular shape, as shown in Fig. 2. The close structural similarity of the defect lines in the first Cu layer to the periodic lines in the second layer points to a common physical origin.

Upon annealing to higher temperatures (1000 K), the rather disordered lines observed in the second-layer islands in Fig. 1 are transformed into well-ordered structures with parallel line pairs stretching linearly over several hundred angstroms (see Fig. 3). Although the imaged area is dominated by a single orientation of these line pairs, three rotational domains with different orientations are seen to coexist. (In the domain at the center part of the image the line pairs are oriented almost parallel to the scan direction, and the resolution is degraded due to interference effects in the STM measurement.) The transition between different domains occurs by a correlated bending of the parallel lines by 120°. From the known

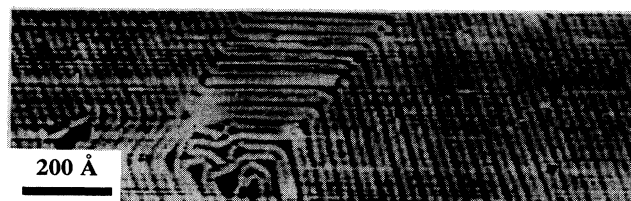


FIG. 3. STM topograph (1500×500 Å²) of a Cu-covered Ru(0001) surface after annealing to 1000 K ($\Theta_{Cu} \approx 2$ ML), exhibiting large, well-ordered domains of the reconstructed Cu bilayer phase. Three different rotational domains are resolved.

orientation of the sample, as determined by LEED, the line pairs proceed in $[120]$ directions, i.e., orthogonal to the close-packed lattice directions. The distance between neighboring line pairs is about 46 \AA , while lines within a pair are about 19 \AA apart. The wider minima between the line pairs are around $0.2\text{--}0.4 \text{ \AA}$ deep, the minima between the lines of a pair are more shallow. No additional corrugation was resolved along the lines.

This corrugation pattern very much resembles that resulting from the contraction of the uppermost layer in the reconstructed Au(111) surface,^{7,8} and can be understood in terms of an equivalent structure, as illustrated in Fig. 4. The Cu atoms in the second layer are contracted along $[100]$ such that 18 second-layer Cu atoms are distributed along 17 atomic spacings of the Ru lattice, with the Cu atoms changing periodically between fcc and hcp stacking. The Cu atoms in the transition regions reside on quasibrige sites and therefore appear raised relative to those on threefold-hollow sites. Hence the elevated lines correspond to transition regions between fcc and hcp stacking ("partial dislocation lines"). This structure leads to a distance of 46.0 \AA between adjacent line pairs, in very good agreement with the measured separation. The different widths of the two kinds of minima indicate different stabilities for fcc and hcp stacking of the Cu atoms, closely resembling observations on Au(111).^{7,8} The stacking type of the respective minimum regions can be deduced from the sequence of line pairs at the boundary between reconstructed second layer and pseudomorphic first layer in the middle-terrace level in Fig. 1. The wider minimum areas in the reconstructed phase directly transform into the pseudomorphic structure, while the narrow minima are separated by a dislocation line from that phase. Hence assuming hcp stacking in the pseudomorphic first layer, as determined in a LEED intensity structural analysis,⁹ the wider minima must correspond to more stable fcc stacking regions.

The presence of a unidirectional contraction contrasts the earlier structural proposal of an isotropically contracted, epitaxial Cu(111) structure in the second layer.^{4,5} It should be noted that, although the contraction along $[001]$ leads to an effective rotation of the close-packed rows of

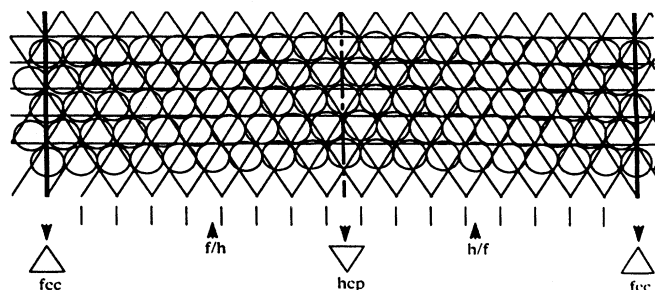


FIG. 4. Top-view model of the atomic structure of the unidirectionally contracted second Cu layer (hexagonal grid: positions of the Cu atoms in the first pseudomorphic layer; large circles: second-layer Cu atoms). The alternating occupation of hcp and fcc threefold-hollow sites requires lateral displacements along $[120]$.

second layer Cu atoms along $[010]$ with respect to the substrate atoms, the $[\sqrt{3} \times \sqrt{3}]$ unit cell of this structure is not rotated compared to the substrate lattice directions. For a rotated unit cell a corrugation along the dislocation lines would be expected, which was not observed. The contraction results in an average Cu-Cu distance of 2.55 \AA along $[001]$, which is practically identical to the interatomic spacings in Cu(111). In the other lattice direction, along the dislocation lines, the Cu-Cu distances are much less affected by the contraction. The distance of 2.67 \AA between nn atoms along the close-packed $[010]$ direction is still close to that of the Ru substrate (2.70 \AA).

The triangular defects in the first layer are associated with domain boundaries. The lines represent partial dislocation lines in the pseudomorphic first layer which mark the transition from the hcp stacking regions in that layer⁹ to fcc domains inside the individual triangles [Fig. 2(b)], and follow the close-packed lattice directions. The 180° change in orientation between subsequent Ru terraces results from the orientation of hcp sites in subsequent layers of an hcp lattice. The fcc domains, which are statistically formed upon Cu deposition at 300 K , are thermodynamically unstable and removed upon annealing to 1000 K . Even at room temperature they are limited in size. Larger domains are not stabilized and split up into a central hcp domain surrounded by three fcc domains, which together form a new triangular structure and can cluster into extended networks of hcp and fcc domains [Fig. 2(b)].

All of these structures can be understood in the framework of the dislocation model for misfit accommodation by Frank and van der Merwe.¹ In the pseudomorphic first layer of Cu adatoms, the corrugation of the adsorption potential for Cu atoms on a Ru(0001) substrate dominates and the Cu atoms are forced into the potential minima given by the substrate. In this layer the Cu atoms are isotropically expanded by 5.5% as compared to the bulk Cu(111) structure. A strong interaction between Ru and adsorbed Cu is reflected by the much higher desorption temperature of the first Cu layer as compared to desorption from subsequent layers.³ The observation of fcc domains in the first Cu layer indicates that adsorption of Cu atoms on fcc and hcp sites is energetically not very different.

In the second Cu layer the cohesive energy between the Cu atoms within that layer dominates and the Cu lattice is contracted. This contraction, however, is not isotropic. The Cu lattice is contracted only in one direction, by 5.5% along $[100]$. Isotropic contractions on a hexagonal substrate, in contrast, were reported for Pd films on Au(111), where a hexagonal network of dislocations is observed.¹⁰ For noble-gas adlayers, e.g., Xe/Pt(111), a transition from a unidirectionally contracted (SI) phase into an isotropically contracted (HI) phase (SI \rightarrow HI transition) was observed upon slight coverage increases.¹¹ The one-dimensional model studies by Frank and van der Merwe and of subsequent authors allowed no distinction between these two contraction types. Two-dimensional calculations led Villain and Gordon to the conclusion that a unidirectional contraction is more favorable in systems with significant repulsions between the dislocation lines.¹² Based on results of their elastic model calculation,

Okwamoto and Bennemann, in contrast, see a unidirectional contraction to be more favorable if the two stacking types, i.e., fcc and hcp stacking, are sufficiently different in energy.¹³ For the unidirectional contraction the ratio of the two stacking areas can be different, which is not possible for an isotropic contraction. This explanation agrees well with the observation of different widths of the fcc and hcp stacking regions. On the other hand, isotropic contractions, where the lattice strain can be removed more evenly, are increasingly favorable for stronger cohesive forces within the layer, as demonstrated by the SI \rightarrow HI transition in Xe/Pt(111).¹¹ On a larger scale, lattice strain can be further reduced within the unidirectionally contracted structure by formation of coexisting rotational domains with different orientations, as observed also on

the reconstructed Au(111) surface.⁸ For thicker films, an effective isotropic contraction must be achieved so that the lattice can finally reach the Cu(111) geometry.

In summary we have shown, by STM measurements, that the lattice strain at the Ru(0001)-Cu interface is partly relieved by a structural transition between a more tightly bound, pseudomorphic first Cu layer and a unidirectionally contracted second layer. These data provide direct proof for a two-dimensional epitaxial structure following the one-dimensional dislocation model by Frank and van der Merwe with periodic sequences of parallel misfit dislocations.

This work was supported by the Deutsche Forschungsgemeinschaft via SFB 338.

¹F. C. Frank and J. H. van der Merwe, Proc. R. Soc. London **198**, 205 (1949).

²K. Yagi, K. Tobayashi, Y. Tanishiro, and K. Takayanagi, Thin Solid Films **126**, 95 (1985).

³K. Christmann, G. Ertl, and H. Shimizu, Thin Solid Films **57**, 247 (1979); J. Catal. **61**, 397 (1980).

⁴J. E. Houston, C. H. F. Peden, D. S. Blair, and D. W. Goodman, Surf. Sci. **167**, 427 (1986).

⁵C. Park, E. Bauer, and H. Poppa, Surf. Sci. **187**, 86 (1987).

⁶G. Pötschke, J. Schröder, C. Günther, R. Q. Hwang, and R. J. Behm, Surf. Sci. (to be published).

⁷C. Wöll, S. Chiang, R. J. Wilson, and P. H. Lippel, Phys. Rev. B **39**, 7988 (1989).

⁸J. V. Barth, H. Brune, G. Ertl, and R. J. Behm, Phys. Rev. B **42**, 9307 (1990).

⁹H. Davies, in *The Structure of Surfaces III*, edited by S. Y. Tong, M. A. van Hove, and X. Xide (Springer, Berlin, in press).

¹⁰K. Yagi, K. Takayanagi, K. Kobayashi, and G. Honjo, J. Cryst. Growth **9**, 84 (1971).

¹¹K. Kern, R. David, P. Zeppenfeld, R. L. Palmer, and G. Comsa, Solid State Commun. **62**, 391 (1987).

¹²J. Villain and M. B. Gordon, Surf. Sci. **125**, 1 (1983).

¹³Y. Okwamoto and K. H. Bennemann, Surf. Sci. **186**, 511 (1987).

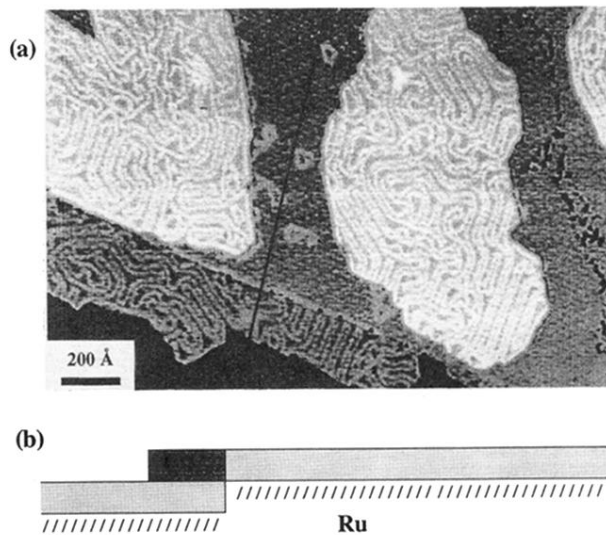


FIG. 1. (a) STM topograph of a Cu-covered Ru(0001) surface ($\Theta_{\text{Cu}}=1.3$, $T_{\text{ann}}=520$ K, $1950 \times 1350 \text{ \AA}^2$) exhibiting three terrace levels (colored light, medium, and dark). A characteristic corrugation on part of the surface and structural defects are resolved. (b) Film/substrate morphology along the line indicated in (a) (Ru substrate: $//////$; 1st Cu layer: $====$; 2nd Cu layer: $■■■■$).

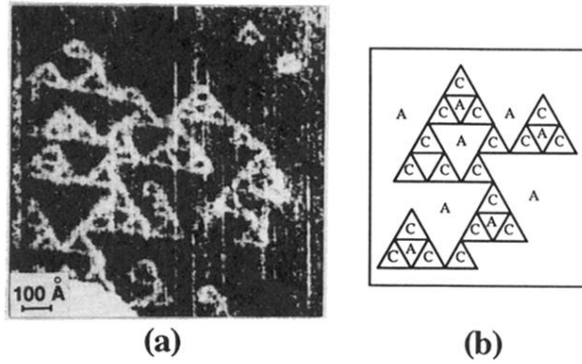


FIG. 2. Defect structure in the first Cu layer on Ru(0001) ($\Theta_{\text{Cu}}=1.3$ ML, $T_{\text{ann}}=520$ K). (a) STM topograph (ca. $1100 \times 1100 \text{ \AA}^2$) resolving a characteristic network of prominent triangles; (b) schematic model indicating the stacking type of Cu atoms in the triangles; *A*: hcp stacking; *C*: fcc stacking.

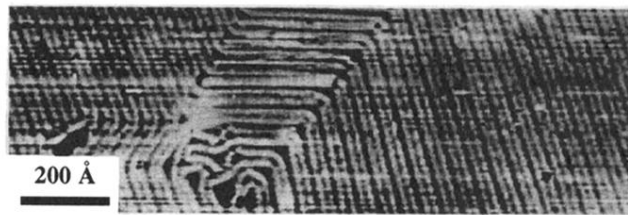


FIG. 3. STM topograph ($1500 \times 500 \text{ \AA}^2$) of a Cu-covered Ru(0001) surface after annealing to 1000 K ($\Theta_{\text{Cu}} \approx 2 \text{ ML}$), exhibiting large, well-ordered domains of the reconstructed Cu bilayer phase. Three different rotational domains are resolved.